

<https://doi.org/10.15407/ujpe66.4.303>

V.I. VISHNYAKOV

Physical-Chemical Institute for Environment and Human Protection,
Min. Edu. Sci. and Nat. Acad. of Sci. of Ukraine
(3, Preobrazhenska Str., Odesa UA-65082, Ukraine; e-mail: eksvar@ukr.net)

IONIZATION BALANCE IN LOW-TEMPERATURE PLASMAS WITH NANOSIZED DUST

Ionization mechanisms in the low-temperature thermal plasma, which contains alkali metal atoms as ionizable component and nanosized dust grains, are studied. In such a plasma, electrons are captured by dust grains, because the work function of grains depends on their sizes, and the electron adsorption rate is more than the thermionic emission rate for nanosized grains. Accordingly, an increase of the dust grain number leads to a decrease in the volume ionization and recombination rates, because they depend on the number density of electrons. At the same time, the role of surface processes in the plasma ionization balance is increased, because the total grain surface is increased. The approximate calculation techniques for low and high grain number densities are proposed. The criterions for approximate calculations are specified.

Keywords: dusty plasmas, surface ionization, thermionic emission.

1. Introduction

The low-temperature atmospheric-pressure thermal plasma consists of electrons, single charged positive ions, ionizable atoms, and a neutral non-interacting buffer gas. The ionization balance in such a plasma without external source is determined by the electron impact ionization of atoms and the electron-ion recombination and is described by the Saha equation [1]:

$$\frac{n_e n_i}{n_a} = \frac{\Sigma_i}{\Sigma_a} \nu_e \exp \frac{-I}{k_B T} \equiv K_S, \quad (1)$$

where n_e , n_i , and n_a are the averages for local thermodynamic equilibrium (LTE) region number densities of electrons, ions, and ionizable atoms, respectively; $n_a = n_A - n_i$, n_A is the number density of atoms available for the ionization; Σ_i and Σ_a are the ion and atom statistical weights; $\nu_e = 2(m_e k_B T / 2\pi \hbar^2)^{3/2}$ is the effective density of elec-

tron states; I is the ionization potential of an atom; k_B is the Boltzmann constant; T is the Kelvin temperature; m_e is the electron mass; \hbar is the Planck constant; K_S is the Saha constant. The condition of neutrality in this case is $n_e = n_i = n_0$, where n_0 is the unperturbed number density, and

$$n_0^2 = (n_A - n_0) K_S.$$

The presence of dust grains in plasma causes the ionization balance displacement. For the first time, Calcote [2] and, later, other researchers [3, 4] observed the abnormal high ionization of rich hydrocarbon flames. Shuler and Weber [4] assumed that the source of the excess ionization is the electrons emitted from the surface of carbon particles. Einbinder [5] proposed a description of the plasma ionization, based on the equilibrium of submicron particles with plasma. This method has been modified by Arshinov and Musin [6, 7] in the case of negatively charged particles. They have obtained the equilibrium constant as a function of the particle size and charge

distribution. Gibson [8] proposed the numerical modeling of the ionization balance at the thermionic emission. The further studies, including up-to-date ones, are basically devoted to the determination of the electron number density and dust grain charges [9–15].

The ionization balance in a dusty plasma was studied insufficiently. The effects of thermionic and ion emissions from dust grains on the ionization state of the hot gas was considered in Ref. [16] for the problem of the evolution of protoplanetary disks. This consideration also demonstrates that the electron and ion number densities increase. However, the dusty plasma in flames and welding fumes is a result of metal's (metal oxide's) vapor condensation and can contain nanosized particles (liquid nuclei) with a very high number density, which provide the intense interphase interaction and electrons' adsorption by dust [17, 18]. The Saha equation is inapplicable in this case, because the additional channels for atom ionization/recombination and electron emission/adsorption are appeared.

The presented paper is devoted to the description of the ionization balance in thermal dusty plasmas with intense processes on the interphase boundary as a function of dust grains' number density. The ionization balance determines the equilibrium electron and ion average number densities, which are provide the plasma conductivity and dust grains' charging and are necessary for any plasma application. The local thermodynamic equilibrium approach is used, i.e. the system is considered as isothermal with absolute temperature about 2000–3000 K, which is usual for the flames and welding fumes. The modeling of the formation of primary particles in welding fumes [19, 20] is used for the calculation of the ionization balance and nucleation.

2. Ionization and Recombination Rates

The Saha equation (1) describes the volume ionization via gas particles' collisions. Electron-atom collisions are described by the electron thermal velocity $v_{Te} = \sqrt{8k_B T / \pi m_e}$ and the collision cross-section πr_a^2 , where r_a is the atom radius, which determines the ionization rate constant $k_{ion} = \pi r_a^2 v_{Te}$ [1]. Therefore, the ionization rate via electron-atom collisions is determined by following equation:

$$\frac{dn_{e(i)}}{dt} = n_e n_a k_{ion} \equiv Q_V^{ion}. \quad (2)$$

The electron-ion recombination in plasma usually occurs as a three-body interaction, when two electrons collide near an ion, and one of them loses the kinetic energy and is captured by the ion. The three-body recombination rate is described as

$$\frac{dn_{e(i)}}{dt} = n_e^2 n_i k_{rec} \equiv Q_V^{rec}, \quad (3)$$

where $k_{rec} = k_{ion}/K_S$ is the recombination rate constant.

The balance of equations (2) and (3) leads to the Saha equation (1) for the plasma without interphase interaction.

However, the presence of dust grains creates additional channels for the appearance and disappearance of charge carriers at the expense of the phase boundary, which causes the thermionic emission, electron adsorption, surface atom ionization, and ion recombination.

The plasma ions and atoms have sporadic collisions with dust grains, which cause the surface atom ionization and ion recombination. The surface ionization balance is determined by the ratio of ion (n_{is}) to neutral atom (n_{as}) number densities at the grain surface, which is described by the well-known Saha–Langmuir equation [21]:

$$\alpha_s = \frac{n_{is}}{n_{as}} = \frac{\sum_i}{\sum_a} \exp \frac{W_d - I}{k_B T},$$

where W_d is the work function of a dust grain with regard for the dependence of the work function on the grain radius [22]: $W_d = W + 0.39e^2/r_d$; W is the work function of a material; r_d is the grain radius.

The neutral atoms are adsorbed by the dust grain surface via collisions with the cross-section $\sigma_{ad} = \pi r_d^2$, and there exists a probability of the electron transition between a valence electron level in the atom and the Fermi level in the dust, which is determined by the ratio $\alpha_s/(1 + \alpha_s)$ [16]. The activation energy ε_i is necessary for the ion desorption [23], and the constant for the atom surface ionization can be defined as $\beta_s = \alpha_s(1 + \alpha_s)^{-1} \exp(-\varepsilon_i/k_B T)$. The positive ion must overcome the attraction of a negatively charged grain for leaving it, which is determined by potential barrier on the plasma-grain boundary [19]

$$V_b = \frac{r_D k_B T}{2r_d} \operatorname{arsinh} \frac{2e^2 Z_d}{r_D k_B T},$$

where Z_d is the dust grain charge number, $r_D = \sqrt{k_B T / 8\pi e^2 n_0}$ is the Debye screening length. In

the system under consideration, the increase of n_d leads to the Coulomb approach applicability: $V_b = e^2 Z_d / r_d$.

Therefore, the activation energy $\varepsilon_i = -V_b$ and the surface ionization constant

$$\beta_s = \frac{\alpha_s}{1 + \alpha_s} \exp \frac{V_b}{k_B T}, \quad V_b < 0.$$

Then the rate of atom ionization on the grain surface is

$$Q_s^{\text{ion}} = n_a n_d \sigma_{ad} v_{Ta} \beta_s, \quad (4)$$

where n_d is the dust grain number density; $v_{Ta} = \sqrt{8k_B T / \pi m_a}$ is the atom thermal velocity, m_a is the atom mass.

The rate of ion recombination on the grain surface is

$$Q_s^{\text{rec}} = n_i n_d \sigma_{id} v_{Ti} \gamma_s, \quad (5)$$

where $v_{Ti} \cong v_{Ta}$ is the ion thermal velocity; $\gamma_s = (1 + \alpha_s)^{-1}$ is the surface recombination constant; σ_{id} is the ion-grain collision cross-section [14]:

$$\sigma_{id} = \pi r_d^2 \left(1 - \frac{V_b}{k_B T} \right).$$

The thermionic emission is determined by the Richardson equation

$$j_e^T = \frac{4\pi m_e (k_B T)^2}{(2\pi\hbar)^3} \exp \frac{-W_d}{k_B T} = \frac{1}{4} \nu_e v_{Te} \exp \frac{-W_d}{k_B T},$$

and the thermionic emission rate is

$$Q_e^T = \pi r_d^2 n_d \nu_e v_{Te} \exp \frac{-W_d}{k_B T}. \quad (6)$$

The electron adsorption rate via sporadic collisions is

$$Q_e^{\text{ads}} = n_e n_d \sigma_{ed} v_{Te}, \quad (7)$$

where σ_{ed} is the electron-grain collision cross-section [14]:

$$\sigma_{ed} = \pi r_d^2 \exp \frac{V_b}{k_B T}.$$

It should be noted, that the collisionless approach is used here, because, in air with a temperature of 3000 K, the mean free paths of electrons ($\lambda_e \sim 5 \mu\text{m}$) and ions ($\lambda_i \sim 1 \mu\text{m}$) are greater than the screening length ($r_D \sim 40 \text{ nm}$) and the grain size.

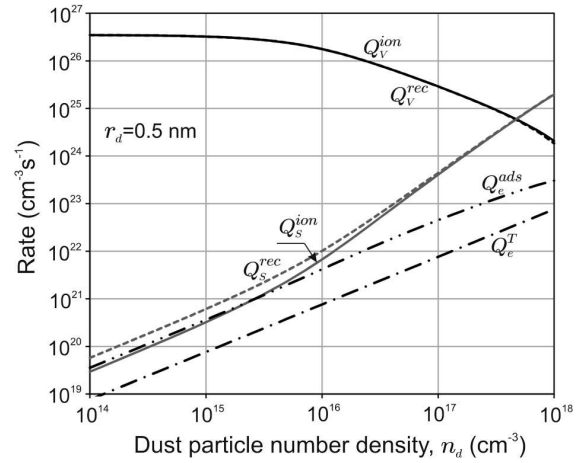


Fig. 1. Dependences of the rates on the grain number density for potassium ionizable atoms and the dust grain radius $r_d = 0.5 \text{ nm}$

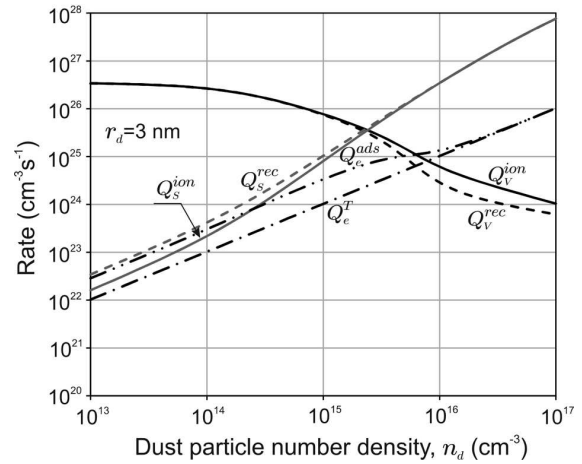


Fig. 2. Dependences of the rates on the grain number density for potassium ionizable atoms and the dust grain radius $r_d = 3 \text{ nm}$

The rates of surface processes, which provide the equilibrium state, depend on the dust grain number density. The example of such dependences is presented in Fig. 1 for potassium ($I = 4.3 \text{ eV}$) ionizable atoms with the initial number density $n_A = 10^{18} \text{ cm}^{-3}$, which provides the Saha unperturbed number density $n_0 = 4.5 \times 10^{15} \text{ cm}^{-3}$ at the temperature $T = 3000 \text{ K}$. The work function of majority metals is in the interval 4–5 eV. Therefore, the value $W = 4.5 \text{ eV}$ was chosen for calculations with regard for the dependence of the work function on the grain radius. The dust grain radius $r_d = 0.5 \text{ nm}$. Accordingly, the work function $W_d = 5.6 \text{ eV}$.

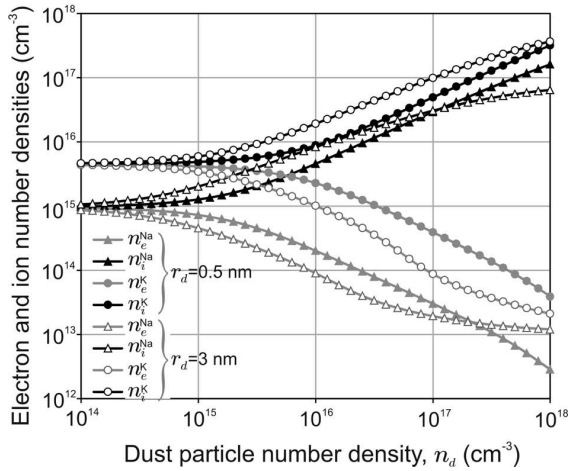


Fig. 3. Dependences of n_i (black) and n_e (grey) on the grain number density for potassium (circle) and sodium (triangle) ionizable atoms with the initial number density $n_A = 10^{18} \text{ cm}^{-3}$

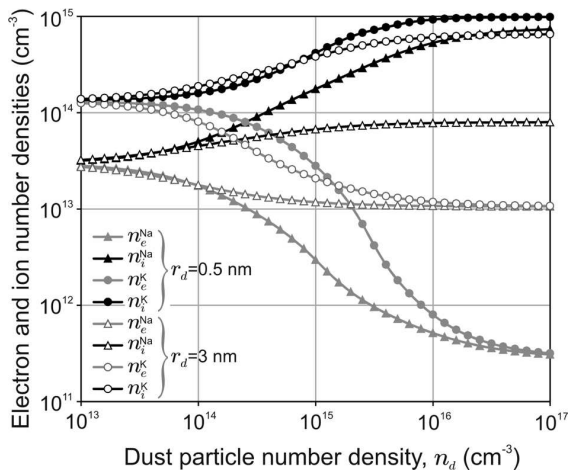


Fig. 4. Dependences of n_i (black) and n_e (grey) on the grain number density for potassium (circle) and sodium (triangle) ionizable atoms with the initial number density $n_A = 10^{15} \text{ cm}^{-3}$

The same dependences for the grain radius $r_d = 3 \text{ nm}$ and the work function $W_d = 4.7 \text{ eV}$ are presented in Fig. 2.

3. Electron and Ion Number Densities

Thus, the ionization balance in a dusty plasma should be determined by separate equations for electrons and ions with regard for the volume (Eqs. (2), (3)) and surface (Eqs. (4)–(7)) processes:

$$Q_V^{\text{ion}} + Q_e^T = Q_V^{\text{rec}} + Q_e^{\text{ads}}, \quad (8a)$$

$$n_e k_{\text{ion}} \left(n_a - \frac{n_e n_i}{K_S} \right) = \pi r_d^2 n_d v_{Te} \times \left(n_e \exp \frac{V_b}{k_B T} - \nu_e \exp \frac{-W_d}{k_B T} \right), \quad (8b)$$

$$Q_V^{\text{ion}} + Q_s^{\text{ion}} = Q_V^{\text{rec}} + Q_s^{\text{rec}}, \quad (9a)$$

$$n_e k_{\text{ion}} \left(n_a - \frac{n_e n_i}{K_S} \right) = \pi r_d^2 n_d v_{Ti} \frac{1}{1 + \alpha_s} \times \left[n_i \left(1 - \frac{V_b}{k_B T} \right) - n_a \alpha_s \exp \frac{V_b}{k_B T} \right], \quad (9b)$$

which should be added by the neutrality equation [14]

$$n_e = n_i + Z_d n_d. \quad (10)$$

The dependences of the equilibrium average electron and ion number densities on the grain number density are presented in Fig. 3 for potassium and sodium ionizable atoms with the initial number density $n_A = 10^{18} \text{ cm}^{-3}$, temperature $T = 3000 \text{ K}$, and grain radii of 0.5 nm and 3 nm . The same dependences for the initial number density $n_A = 10^{15} \text{ cm}^{-3}$ are presented in Fig. 4. The Muller method is used for calculations.

The increase of the dust grain number leads to the volume ionization. The recombination rates decrease, because they depend on the number density of electrons (see Eqs. (2) and (3)), which are captured by grains.

The ionizable atom number density strongly influences the ionization balance displacement via surface processes. It is illustrated by Fig. 5. Such dependences were discussed in details in Refs. [11, 24]. At low n_A , the plasma presents a system of positively charged dust grains and electrons emitted by them. Such a plasma can be described as the dust-electron plasma [25, 26]. At a very high ionizable atom number density, the presence of dust has a little effect on the electron number density. The values of n_e and n_i are close to the unperturbed (Saha) number density n_0 . At intermediate n_A , a reversal of the grain charge occurs; the electrons are adsorbed by dust and $n_i \gg n_e$.

4. Discussion

Solving the balance equations (8) and (9) demonstrates a decrease in the electron number density, while the grain number density increases. The electrons are captured by dust grains, because their adsorption rate is greater than the thermionic emission

rate. When plasma contains a small number of the dust grains, the ionization and recombination rates via electron-atom and electron-ion collisions are defined. In this case, the average electron number density can be determined by the Saha equation (1) with neglected inhomogeneity in the space charge layer near the grain surface. However, the ion number density should be calculated with regard for the surface ionization by using the expression $Q_s^{\text{ion}} \cong Q_s^{\text{rec}}$:

$$n_i \cong \frac{n_A \alpha_s}{\left(1 - \frac{V_b}{k_B T}\right) \exp \frac{-V_b}{k_B T} + \alpha_s}, \quad (11)$$

$$n_e \cong \nu_e \left(1 - \frac{V_b}{k_B T}\right) \exp \frac{-W_d - V_b}{k_B T}, \quad (12)$$

$$V_b = \frac{e^2(n_e - n_i)}{r_d n_d}. \quad (13)$$

The comparison of the numerical solutions of the full system (8)–(10) and system (11)–(13) gives the following criterion for this approach (with a discrepancy less of 10%):

$$n_d \leq 35 \frac{n_0}{r_d^2} \text{ nm}^2.$$

The high number density of dust is observed in the systems, where the condensation of metal (metal oxide) vapors occurs. The nucleation in the cooling (as a result of the mixing of hot vapors with air) thermal plasma [27, 28] provides a much greater nucleus number density than the number densities of charge carriers [29]. The heterogeneous ion-induced nucleation occurs, while the activation energy of the growth exists, which decreases down to zero under the cooling of plasma. After that, the nucleation transfers into the unrestricted growth of nuclei via the vapor condensation and coagulation [30].

When the grain number density

$$n_d \geq 300 \frac{n_0}{r_d^2} \text{ nm}^2,$$

Eq. (12) should be replaced by the following equation

$$n_e \cong \nu_e \exp \frac{-W_d - V_b}{k_B T}, \quad (14)$$

because the detailed balance in surface processes ($Q_e^T \cong Q_e^{\text{ads}}$) is applicable in this case.

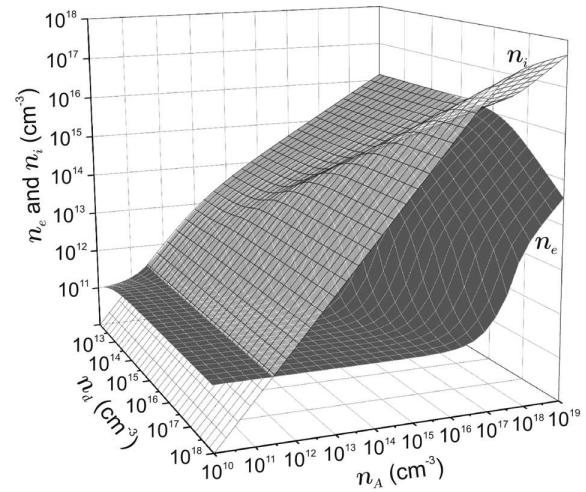


Fig. 5. Dependences of n_e (black) and n_i (white semitransparent) on the potassium initial atom and dust grain number densities; the grain radius $r_d = 0.5$ nm

In the transition interval of grain number densities

$$35 < \frac{n_d r_d^2}{n_0} \text{ nm}^{-2} < 300,$$

Eqs. (8) and (9) should be used, though Eq. (11) for the ion number density remains valid in the transition interval.

The detailed balance between the thermionic emission and electron adsorption is applicable for any dust number at the low atom number density (see Fig. 2). In this case, the potential barrier $V_b \ll k_B T$, Eq. (12) becomes equal to Eq. (14) and $Q_e^{\text{ads}} \cong Q_e^T$ even at low n_d . An increase of the dust number density causes a decrease of the volume collision ionization. Therefore, the electron number density remains a constant, as the atom number density increases up to a limit, which is determined by the grain number density (see Fig. 5).

The volume thermal ionization is the basic process at the low number density of dust grains; however, the ionization mechanism is replaced by the surface ionization at the high dust grain number. The investigation of the Poisson–Boltzmann equation [31] demonstrates that the unperturbed number density can be determined as $n_0^* = \sqrt{n_e n_i}$, which equals the unperturbed Saha number density n_0 in the plasma without dust. The change of the ionization mechanism can be illustrated by the dependences of the ratio $\sqrt{n_e n_i}/n_0$ on the grain number density, which are presented in Fig. 6.

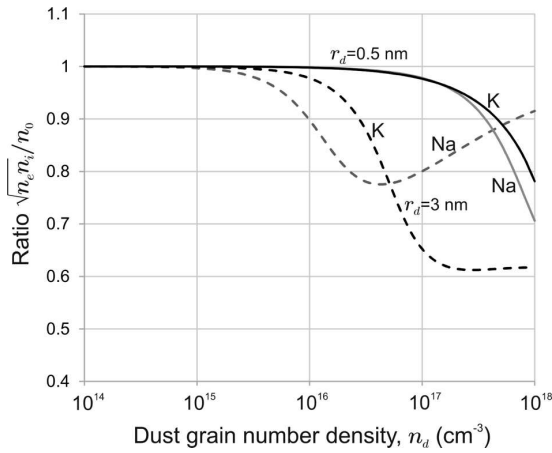


Fig. 6. Dependences of the unperturbed number density on the grain number density for potassium (black) and sodium (grey) ionizable atoms

In the case where the volume ionization can be neglected, the unperturbed number density is described by the equation

$$n_0^{*2} = n_e n_i \cong n_a K_S \left(1 - \frac{V_b}{k_B T}\right)^{-1}, \quad (15)$$

which gives the unperturbed number density smaller than that from the Saha equation (1).

The average charge of grains is inversely proportional to their number density; therefore, its absolute value decreases, as the grain number increases, and causes a decrease of the potential barrier absolute value. Thus, the value in brackets in Eq. (15) tends to 1, when the grain number density is increased. Therefore, unperturbed number density tends to the Saha value at the very great numbers of dust grains, because only one of many grains has a charge $Z_d = -1$, others are neutral; and a displacement of the ionization balance takes place only near these charged grains, and another part of plasma can be described by the Saha equation.

Accordingly, the surface ionization, which is described by Eq. (4), occurs only near these dust grains. This is well illustrated in Fig. 4, where the saturation of ion number densities with increase of the grain number density is demonstrated.

An increase of the ionization potential of an atom reinforces the effect of the surface ionization on the ionization balance. The equilibrium unperturbed number density for sodium ($I = 5.1$ eV) ionizable atoms with the initial number density $n_A = 10^{18} \text{ cm}^{-3}$, calculated by the Saha equation, $n_0 =$

$= 9.6 \times 10^{14} \text{ cm}^{-3}$ at the temperature $T = 3000$ K. In this case, the Saha number density less than for the potassium and surface processes begins to influence the volume ionization at the smaller value of the grain number density. This fact correlates with experimental data from Ref. [32], where the effect of a potassium additional agent ($I = 4.3$ eV) on the nucleation in the plasma with iron atoms ($I = 7.9$ eV) as a predominant ionizable component was studied. The theoretical model of nucleation, which explains this effect by the surface ionization, is presented in Ref. [18].

5. Conclusion

The ionization balance in a thermal plasma without external sources of ionization is determined by the Saha equation, which describes the ionization and recombination via collisions between gas particles. This description remains applicable in a dusty thermal plasma at the small number of dust grains. However, the surface atom ionization ion recombination, thermionic emission, and surface electron adsorption become the predominant processes at the large dust grain number.

The surface processes begin to play an essential role, if the grain number density becomes greater than $50 (n_0/r_d^2) \text{ nm}^2$. It should be noted that the grain number densities, which were used in the present consideration, could be applied only for nano-sized grains, because the average distance between them is $\sim 12 \text{ nm}$ for $n_d = 10^{18} \text{ cm}^{-3}$.

The ionization potential of an atom also influence the competition between the volume and surface ionizations. An increase of the ionization potential provides a decrease of the ionization degree, i.e. a decrease of the unperturbed number density. Thus, the surface ionization begins to replace the volume ionization at the smaller value of the grain number density.

For low and high dust grain number densities, the approximate calculation techniques are proposed. For a low dust grain number density, the average electron number density can be determined by the Saha equation. For a high dust grain number density, the average electron number density is determined by the detailed balance in surface processes. The ion number density should be calculated by using the Saha–Langmuir equation in any case.

1. M. Mitchner, C.H. Kruger. *Partially Ionized Gases* (Wiley, 1973) [ISBN: 978-0471611721].

2. H.F. Calcote, R.N. Pease. Electrical properties of flames. Burner flames in longitudinal electric fields. *Ind. Eng. Chem.* **43**, 2726 (1951).
3. T.M. Sugden, B.A. Thrush. A cavity resonator method for electron concentration in flames. *Nature* **168**, 703 (1951).
4. K.E. Shuler, J. Weber. A microwave investigation of the ionization of hydrogen-oxygen and acetylene-oxygen flames. *J. Chem. Phys.* **22**, 491 (1954).
5. H. Einbinder. Generalized equation for the ionization of solid particles. *J. Chem. Phys.* **26**, 948 (1957).
6. A.A. Arshinov, A.K. Musin. Thermionic emission from carbon particles. *Soviet Physics Doklady* **3**, 99 (1958).
7. A.A. Arshinov, A.K. Musin. Equilibrium ionization of particles. *Soviet Physics Doklady* **3**, 588 (1958).
8. E.G. Gibson. Ionization phenomena in a gas-particles plasma. *Phys. Fluids* **9**, 2389 (1966).
9. M.S. Sodha, P.K. Kaw. Field emission from negatively charged solid particles. *J. Phys. D: Appl. Phys.* **1**, 1303 (1968).
10. D.I. Zhukhovitskii, A.G. Khrapak, I.T. Yakubov. Ionization equilibrium in a highly nonideal plasma containing a condensed dispersed phase. *Teplofiz. Vys. Temp.* **22**, 833 (1984) [*High Temp.* **22**, 643 (1985)].
11. I.T. Yakubov, A.G. Khrapak. Thermophysical and electrophysical properties of low-temperature plasma with condensed disperse phase. In: *Soviet Technology Reviews/Section B, Thermal Physics Reviews*. Edited by A.E. Sceindlin, V.E. Fortov (Harwood Academic Publishers, 1989), Vol. 2, P. 269 [ISBN: 3-7186-4909-8].
12. J. Goree. Charging of particles in plasma. *Plasma Sources Sci. Technol.* **3**, 400 (1994).
13. P.K. Shukla, A.A. Mamun. *Introduction to Dusty Plasma Physics* (Institute of Physics, Bristol, 2002) [ISBN: 978-0750306539].
14. V.E. Fortov, A.G. Khrapak, S.A. Khrapak, V.I. Molotkov, O.F. Petrov. Dusty plasmas. *Phys. Uspekhi* **47**, 447 (2004).
15. M.S. Sodha, S.K. Mishra. Validity of Saha's equation of thermal ionization for negatively charged spherical particles in complex plasmas in thermal equilibrium. *Phys. Plasmas* **18**, 044502 (2011).
16. S.J. Desch, N.J. Turner. High-temperature ionization in protoplanetary disks. *Astrophys. J.* **811**, 156 (2015).
17. V.I. Vishnyakov, S.V. Kozytsyi, A.A. Ennan. Change of ionization mechanism in the welding fume plasma from gas metal arc welding. *Aerosol Sci. Engin.* **3**, 49 (2019).
18. V.I. Vishnyakov, S.V. Kozytsyi, A.A. Ennan. Features of nucleation in welding fumes from gas metal arc welding. *J. Aerosol Sci.* **137**, 105439 (2019).
19. V.I. Vishnyakov, S.A. Kiro, M.V. Oprya, O.D. Chursina, A.A. Ennan. Numerical and experimental study of the fume chemical composition in gas metal arc welding. *Aerosol Sci. Engin.* **2**, 109 (2018).
20. V.I. Vishnyakov, S.A. Kiro, M.V. Oprya, A.A. Ennan. Effect of shielding gas temperature on the welding fume particle formation: Theoretical model. *J. Aerosol Sci.* **124**, 112 (2018).
21. M.J. Dresser. The Saha-Langmuir equation and its application. *J. Appl. Phys.* **39**, 338 (1968).
22. B.M. Smirnov. Processes in plasma and gases involving clusters. *Phys. Uspekhi* **40**, 1117 (1997).
23. V.I. Vishnyakov. Probe in the thermal collision plasma. *Phys. Plasmas* **14**, 013502 (2007).
24. V.E. Fortov, I.T. Yakubov. *The Physics of Non-Ideal Plasma* (World Scientific, 2000) [ISBN: 978-0891166047].
25. V.I. Vishnyakov. Thermo-emission (dust-electron) plasmas: Theory of neutralizing charges. *Phys. Rev. E* **74**, 036404 (2006).
26. V.I. Vishnyakov. Charging of dust in thermal collisional plasmas. *Phys. Rev. E* **85**, 026402 (2012).
27. V.I. Vishnyakov. Homogeneous nucleation in thermal dust-electron plasmas. *Phys. Rev. E* **78**, 056406 (2008).
28. V.I. Vishnyakov, S.A. Kiro, A.A. Ennan. Heterogeneous ion-induced nucleation in thermal dusty plasmas. *J. Phys. D: Appl. Phys.* **44**, 215201 (2011).
29. V.I. Vishnyakov, S.A. Kiro, A.A. Ennan. Formation of primary particles in welding fume. *J. Aerosol Sci.* **58**, 9 (2013).
30. V.I. Vishnyakov, S.A. Kiro, A.A. Ennan. Bimodal size distribution of primary particles in the plasma of welding fume: Coalescence of nuclei. *J. Aerosol Sci.* **67**, 13 (2014).
31. V.I. Vishnyakov, G.S. Dragan, V.M. Evtuhov. Nonlinear Poisson-Boltzmann equation in spherical symmetry. *Phys. Rev. E* **76**, 036402 (2007).
32. V.I. Vishnyakov, S.A. Kiro, M.V. Oprya, O.I. Shvets, A.A. Ennan. Nonequilibrium ionization of welding fume plasmas; Effect of potassium additional agent on the particle formation. *J. Aerosol Sci.* **113**, 178 (2017).

Received 30.03.20

В.І. Вишняков

ІОНІЗАЦІЙНА РІВНОВАГА В НИЗЬКОТЕМПЕРАТУРНІЙ ПЛАЗМІ З НАНОРОЗМІРНИМИ ПОРОШИНКАМИ

Досліджено іонізаційні механізми в низькотемпературній термічній плазмі, яка містить атоми лужних металів як іонізуючий компонент, та нанорозмірні пилові порошинки. У такій плазмі електрони захоплюються пиловими порошинками, оскільки робота виходу порошинок залежить від їх розмірів, а інтенсивність адсорбції електронів перевищує інтенсивність термоелектронної емісії для порошинок малого розміру. Відповідно, збільшення концентрації порошинок приводить до зменшення інтенсивності об'ємної іонізації і рекомбінації, так як вони залежать від концентрації електронів. При цьому зростає роль поверхневих процесів у балансі іонізації плазми, оскільки збільшується загальна поверхня порошинок. Запропоновано наближені методи розрахунку для низької і високої концентрації пилових порошинок. Вказано критерії для використання наближених розрахунків.

Ключові слова: запилена плазма, поверхнева іонізація, термoeмісія.